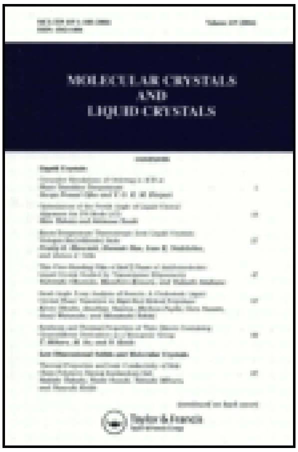

Molecular Crystals and Liquid Crystals Science and Technology. Section A. Molecular Crystals and Liquid Crystals
Publication details, including instructions for authors and subscription information:
http://www.tandfonline.com/loi/gmcl19

Transient Ion Transport in Nematic Liquid Crystals

Shuichi Murakami [a] , Hiroyoshi Naito [a] , Masahiro Okuda [a] & Akihiko Sugimura [b]

[a] Department of Physics and Electronics, University of Osaka Prefecture, 1-1 Gakuen-cho, Sakai, Osaka, 593, Japan

[b] Department of Information Systems Engineering, Osaka Sangyo University, 3-1-1 Nakagaito, Daito, Osaka, 574, Japan

To cite this article: Shuichi Murakami , Hiroyoshi Naito , Masahiro Okuda & Akihiko Sugimura (1995): Transient Ion Transport in Nematic Liquid Crystals, Molecular Crystals and Liquid Crystals Science and Technology. Section A. Molecular Crystals and Liquid Crystals, 263:1, 479-489

To link to this article: http://dx.doi.org/10.1080/10587259508033607

Mol. Cryst. Liq. Cryst. 1995, Vol. 263, pp. 479–489
Reprints available directly from the publisher
Photocopying permitted by license only

TRANSIENT ION TRANSPORT IN NEMATIC LIQUID CRYSTALS

SHUICHI MURAKAMI, HIROYOSHI NAITO and MASAHIRO OKUDA
Department of Physics and Electronics, University of Osaka Prefecture,
1-1 Gakuen-cho, Sakai, Osaka 593, Japan
AKIHIKO SUGIMURA
Department of Information Systems Engineering, Osaka Sangyo University,
3-1-1 Nakagaito, Daito, Osaka 574, Japan

Abstract Transient photocurrent experiments in amorphous selenium and nematic liquid crystal double layers have been carried out to investigate the transient ion transport process in 4-cyano-4'-alkyl-biphenyl. It is found that the mobile charge carriers in the liquid crystal are positive ions with the drift mobility of $3.5 \times 10^{-6} cm^2/Vs$ at $303K$ and have the ionic radius of $0.32nm$. The numerical analysis is also carried out to gain insight into the injection process of photogenerated charge carriers from the amorphous selenium layer into the nematic liquid crystal layer.

§1. INTRODUCTION

Recently, considerable attention has been directed toward the charge carrier transport process in nematic liquid crystals (NLCs).$^{1-7)}$ This arises from the fact that the charge carrier transport process plays an important role in NLC displays.

Knowledge of the drift mobility of the charge carrier is of fundamental importance for proper understanding of the charge carrier transport process. The drift mobility in NLCs has been obtained from transient currents induced by single or bipolar voltage application to NLCs so far.$^{1-3)}$ With these methods, however, we cannot distinguish positive from negative charge carriers which drift through the NLC layer, and cannot determine the drift mobility accurately because it is impossible to check whether or not the transient current is the space-charge limited current (SCLC).$^{8)}$

Time-of-flight (TOF) experiments have been often employed for the study of transient charge transport in a vast class of photoconductive materials.$^{8)}$ The TOF experiment is most easily performed by injecting a thin unipolar carrier sheet at one end of a cell and measuring the transit time it takes for the sheet to drift across the cell under the influence of a dc bias field. Accordingly, by choosing the polarity of the driving field, positive and negative charge carrier transport processes can be studied separately, and an accurate drift mobility can be determined under either small-signal or SCLC conditions.[8)]

To inject a thin unipolar sheet at one end of the cell, the strongly absorbed light is generally used. However, even ultraviolet light is not strongly absorbed in NLCs such as 4-cyano-4'-alkyl-biphenyl (5CB) which is used in our experiment. Hence, amorphous selenium (a-Se) is used as a photocarrier generation layer in this work, where a-Se is an ambipolar photoconductor; electron and hole mobilities are 0.01 and $0.16 cm^2/Vs$ at $300K$, respectively.[9)] Such a charge carrier generation layer (CGL) / charge carrier transport layer (CTL) structure is often used to study the charge carrier transport process in organic materials.[10)] The photogenerated carriers in the a-Se layer are injected into the NLC layer and then drift toward the back electrode. From the transient photocurrents in the a-Se/NLC double layer, we can obtain information concerning the charge carrier transport process in NLCs.

§2. THEORY

2.1. The Injection Process

Injection processes of electronic carriers from a photoconductor to an insulating liquid have been described by Hartmann and Schmidlin.[11)] Figure 1 shows possible injection processes; (a) thermionic transfer, (b) thermally assisted tunneling, (c) trapping in an interfacial state followed by ion desorption. We will show later that the mobile charge carrier in the NLC layer is a positive ion, and thereby we focus on injection process (c) in Fig. 1.

A rate equation for the total number of free holes in the a-Se layer, denoted by N, is

$$\frac{\partial N}{\partial t} = g(t) - \omega_1 N, \tag{1}$$

where $g(t)$ is the photogeneration rate and ω_1 is the capture rate by a neutral molecule adsorbed at the a-Se/NLC interface. The photogeneration rate is written as

$$g(t) = N_{ph}\delta(t), \tag{2}$$

where N_{ph} is the total number of photogenerated charge carriers and $\delta(t)$ is a delta function. The deep trapping or recombination of photogenerated carriers in the a-Se layer is neglected. After the capture of free holes, the neutral molecules are converted to the positive ions at the interface. A rate equation for the density of the ions, N_1, at the a-Se/NLC interface is

$$\frac{\partial N_1}{\partial t} = \omega_1 N - r_d N_1, \tag{3}$$

where r_d is the rate that the created ions desorb into the NLC layer. In this case, the ion flux leaving the interface, f_{inj}, is

$$f_{inj} = r_d N_1. \tag{4}$$

From Eqs. (1)-(4), we obtain

$$f_{inj}(t) = \frac{\omega_1 r_d N_{ph}}{\omega_1 - r_d}[\exp(-r_d t) - \exp(-\omega_1 t)]. \tag{5}$$

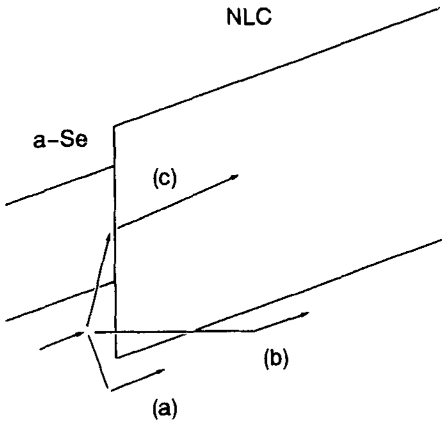

Figure 1. Schematic illustration of injection processes of charge carriers from a-Se to NLC.

2.2. The Transport Process

In the absence of diffusion, the transport of ions in the NLC layer is described by the following equations:

$$J(t) = \mu\rho(x,t)E(x,t) + \epsilon\frac{\partial E(x,t)}{\partial t}, \tag{6}$$

$$\frac{\partial\rho(x,t)}{\partial t} = -\frac{\partial}{\partial x}[\mu\rho(x,t)E(x,t)], \tag{7}$$

$$\frac{\partial E(x,t)}{\partial x} = \frac{1}{\epsilon}\rho(x,t), \tag{8}$$

where $J(t)$ is the total current, μ is the carrier mobility, $\rho(x,t)$ is the density of ions, $E(x,t)$ is the electric field, and ϵ is the permittivity of the NLC layer. Equations (6)-(8) are the equation for total current, the continuity equation, and the Poisson equation, respectively. The transient current is calculated from

$$J(t) = \frac{1}{L}\int_0^L \mu\rho(x,t)E(x,t)dx, \tag{9}$$

where L is the thickness of the NLC layer. Equations (7) and (8) are numerically solved for $\rho(x,t)$ and $E(x,t)$ under the initial conditions, $\rho(x,0) = 0$ and $E(x,0) = V/L$ and the boundary conditon, Eq. (5).

§3. EXPERIMENT

NLC used was 4-cyano-4'-5-alkyl-bipheneyl (5CB), which has a positive dielectric anisotropy $\Delta\epsilon \simeq 10$. The layer thickness of 5CB was $7.0\mu m$. a-Se was chosen as CGL because of its high photosensitivity. The a-Se layer was prepared by vacuum evaporation and was $0.2\mu m$ in thickness. The transient photocurrents of the a-Se/5CB cells were measured with the standard time-of-flight technique.[8)] An external voltage was applied to the cell, and then the a-Se layer was illuminated using a xenon flash lamp with pulse duration of $1\mu s$ and an appropriate optical filter. The light pulse was strongly absorbed and generated electron and hole pairs in the a-Se layer. Dependent on the polarity of the applied voltages, positive or negative charge carrier transport processes can be studied separately.

§4. RESULTS AND DISCUSSION

4.1. Determination of Drift Mobility

Figure 2 shows typical transient photocurrents of 5CB at $303K$, (a) a positive voltage of $+10V$ is applied to the a-Se layer with respect to the NLC layer, and (b) a negative voltage of $-10V$ is applied to the a-Se layer. The initial spike is due to the transit of the photogenerated carriers in the a-Se layer. A current peak at about $12ms$ is observed only when the positive voltage is applied. The current peak is due to the transit of the charge carrier in the NLC layer. When the positive (negative) voltage is applied to the a-Se layer, photogenerated holes (electrons) in the a-Se layer are injected into the NLC layer. Therefore, it is evident from Fig. 2 that the drift mobility of the negative charge carrier in the NLC layer is much smaller than that of the positive charge carrier.

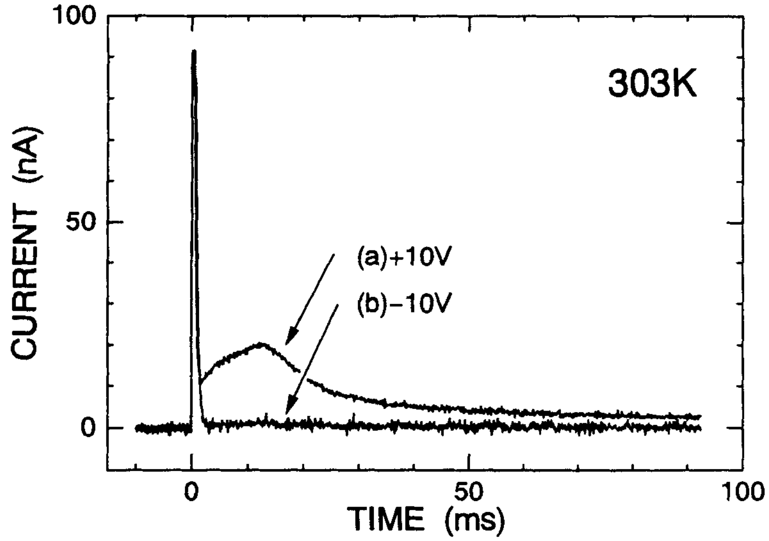

Figure 2. Typical transient photocurrents of an a-Se/5CB cell at $303K$. (a) $+10V$ is applied to the a-Se layer with respect to the 5CB layer, and (b) $-10V$ is applied.

The measurements were made under the SCLC condition to measure the transient photocurrents with better signal-to-noise ratio. Under the condition the current increases owing to the perturbation of the applied field by the excess space charge.

As the carrier sheet moves in the NLC layer, it moves in an increasing field due to the perturbation during the period $0 < t < t_{peak}$, where t_{peak} is the time that the leading edge of the carrier packet reaches the back electrode and is observed as the time at the current peak. The transient currents were measured at different light intensities to confirm that the measurements were carried out under the SCLC condition. Figure 3 shows the relation between the peak time and light intensities. The peak time decreases with increasing light intensity, and the ratio of the peak times at higher light intensities to those at lower light intensities is 0.8.

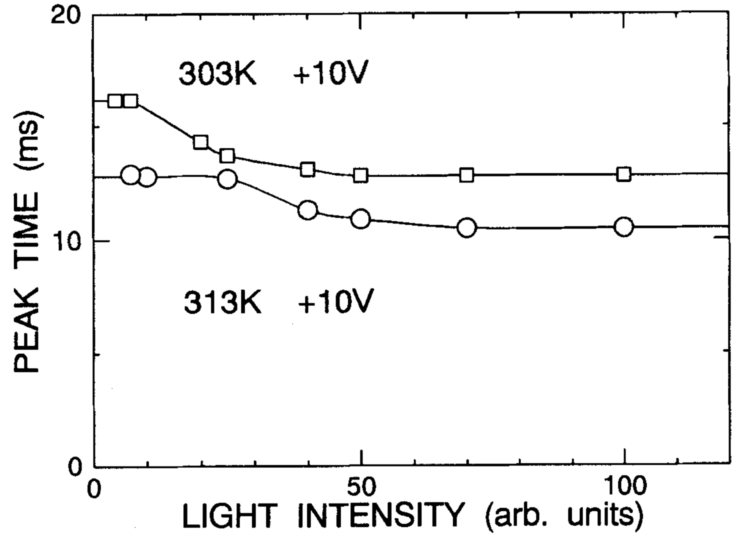

Figure 3. Light intensity dependence of the peak time at $303K$ and $313K$. The applied voltage to the a-Se layer is $+10V$.

In the time region, $0 < t < t_{peak}$, the transient photocurrent in Fig. 2 is concavely curved, while the theoretical transient SCLC in Ref. (12) is convexly curved, implying that the theory for SCLC cannot be directly applied to the experimental data. Then, the transient photocurrent calculated under the SCLC condition according to the theory in Sec. 2 is fitted to the experimental result in Fig. 4. The calculated result is in good agreement with the experimental result. The best-fitted parameters are: $N_{ph} = CV$, $\omega_1 = 12/t_T$, and $r_d = 8/t_T$, where C is the capacitance of the cell, V is the applied voltage, and t_T is the transit transit time. In addition, it is confirmed that the peak time of the calculated current is $0.8t_T$ when the injection current has its maximum value at about $0.1t_T$ as shown in the inset of Fig. 4 (it is called the delay of the injection[13]). Thus, the transit time under the SCLC condition for the injection process (c) in Fig. 1 is obtained from the following relation:

$$t_T = t_{peak}/0.8, \tag{10}$$

which is similar to the relation in Ref. (12).

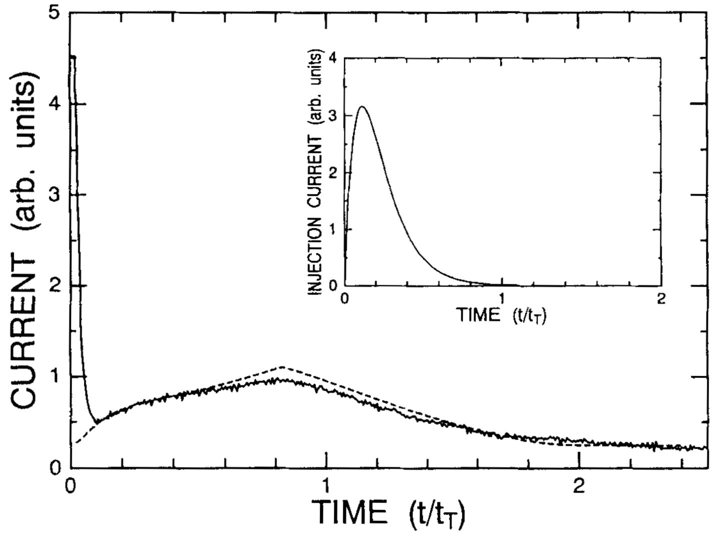

Figure 4. Comparison of the calculated current with the measured current transient. Solid curve is the measured current transient and dushed curve is the calculated transient under the condition that $N_{ph} = CV$, $\omega_1 = 12/t_T$ and $r_d = 8/t_T$, where C is the capacitance of the cell, V is the applied voltage and t_T is the transit time. The inset shows the calculated injection current from the a-Se layer to the NLC layer.

Figure 5 shows a plot of the inverse transit time versus the applied voltage at $303K$ and $313K$. The straight lines can be observed. From the slopes of these lines the drift mobilities are obtained as $3.5\times10^{-6}cm^2/Vs$ at $303K$ and $4.3\times10^{-6}cm^2/Vs$ at $313K$. It is also observed in Fig. 5 that these lines intersect with the abscissa at $2.0V$ and $1.4V$ at $303K$ and $313K$, respectively. The similar phenomena have been observed in the a-Se/p-methoxybenzylidene-p-n-bytylaniline double layer.[7] It was concluded that the voltage was the threshold voltage of the *injection of charge* carriers over the potential barrier formed by the image force in the vicinity of the a-Se/NLC interface.[7] However, the straight lines in Fig. 5 are not expected for this case because the potential barrier formed by the image force is a function of the applied voltage.[11] We, thereby, consider that the threshold voltage is attributable to the built-in potential caused by the adsorbed ionic charges at the a-Se/NLC interface and NLC/electrode interface. The adsorbed ions result from the sweep out of mobile impurity ions in the NLC layer by the applied dc field. Thus, we can estimate the adsorbed charge per unit area to be $1.8\times10^{-9} C/cm^2$.

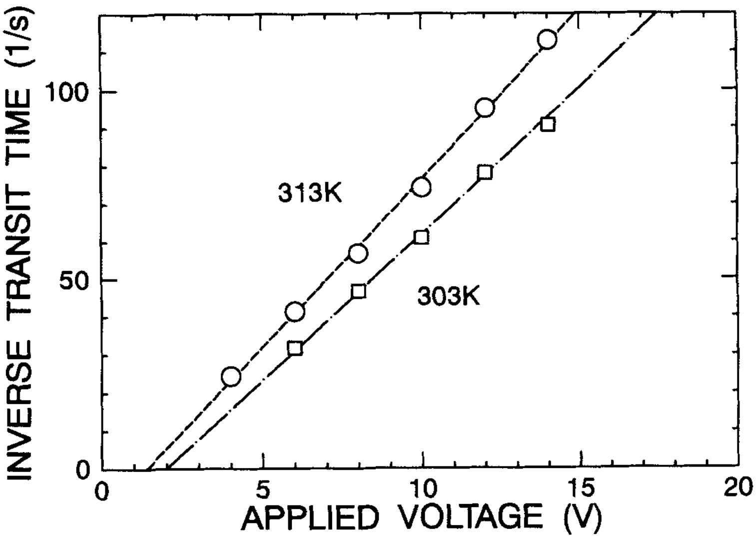

Figure 5. Applied voltage dependences of inverse transit time of positive ions at $303K$ and $313K$.

4.2. Temperature Dependence of Drift Mobility

Figure 6 shows the relation between the drift mobility and the resiprocal temperature. The discontinuity of the drift mobility at T_{NI}, which is the nematic-isotropic point, is observed. In the nematic range, the thermally activated behavior of the drift mobility,

$$\mu = \mu_0 \exp(-E_a/kT),$$

can be seen, where μ is the drift mobilty, k the Boltzman constant, and E_a the activation energy of the drift mobility. The activation energy of the drift mobility in the nematic range is determined to be $0.33eV$.

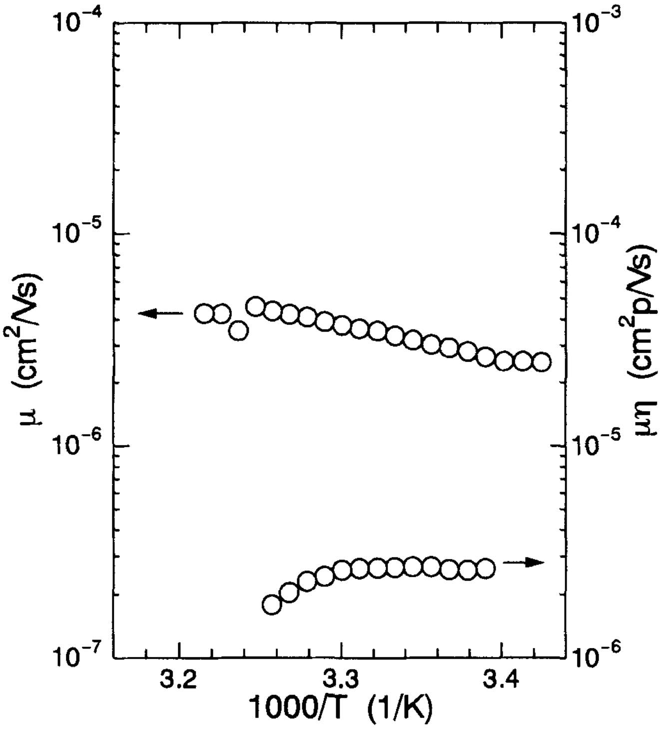

Figure 6. Temperature dependences of the drift mobility of positive ions and of the product of the drift mobility and viscosity of 5CB. The activation energy of the mobility is $0.33eV$. The viscosity of 5CB is taken from Ref. (14).

In Fig. 6, the temperature dependence of the product of the drift mobility which was measured in our experiment, and the viscosity of 5CB reported by Skarp *et al.*,[14] is shown as well. This product is independent of temperature except for the vicinity of T_{NI}, which is known as the Walden rule,

$$\mu\eta = \frac{q}{6\pi r}, \tag{11}$$

where η is the viscosity, and r the ionic radius. If the Walden rule is observed, conduction current is carried by ions.[6] We, therefore, conclude that charge carriers, which drift in the 5CB layer, are ions. The ionic radius is calculated to be $0.32nm$ from Eq. (11). The deviation from the Walden rule in the vicinity of T_{NI} is likely to be due to the pretransitional effect.[15]

§5. CONCLUSIONS

We have carried out the measurements of transient photocurrents in the a-Se/5CB double layers, whose structure enables us to study the photocarrier generation and the transport of charge carriers separately. We observe the transient current shape having a prominent peak under the SCLC condition which is somewhat different from that predicted by the early transient SCLC theory. Hence, we have made the numerical calculation by considering the injection process of photogenerated charge carriers from the a-Se layer into the 5CB layer under the SCLC condition. The numerically obtained transient is in exellent agreement with the experimental one, showing that there exists the delay of the injection of charge carriers at the a-Se/5CB interface, and that the relation between t_T and t_{peak} is $t_T = t_{peak}/0.8$. On the basis of this finding, we can determine the drift mobility of the charge carrier in 5CB; the drift mobilty of the positive charge carrier is obtained as $3.5 \times 10^{-6} cm^2/Vs$ at $303K$. The transit of the negative charge carrier in 5CB has not been observed. The Walden rule is observed in the temperature dependence of the product of the drift mobility and the viscosity. The positive charge carrier in 5CB is therfore an ion, whose radius is calculated to be $0.32nm$.

We further observe the influence of the built-in potential in the 5CB layer on the applied voltage dependence of t_T. We suggest that this potential arises from the adsorption of the ions on the a-Se and electrode surfaces. The adsorbed ion density is estimated to be $1.1 \times 10^{10} cm^{-2}$.

REFERENCES

1) G. H. Heilmeier and P. M. Heyman: Phys. Rev. Lett. 18 (1967) 583.
2) T. Yanagisawa, H. Matsumoto, and K. Yahagi: Jpn. J. Appl. Phys. 16 (1977) 45.
3) A. Sugimura, N. Matsui, Y. Takahashi, H. Sonomura, H. Naito, and M. Okuda: Phys. Rev. B43 (1991) 8272.
4) H. Naito, M. Okuda, and A. Sugimura: Phys. Rev. A44 (1991) 3434.
5) H. Naito, K. Yoshida, M. Okuda, A. Sugimura: J. Appl. Phys. 73 (1993) 1119.
6) K. Yoshino, S. Hisamatsu, and Y. Inuishi: J. Phys. Soc. Jpn. 32 (1972) 867.
7) M. Yamashita and Y. Amemiya: Jpn. J. Appl. Phys. 17 (1978) 1513.
8) F. K. Dolezalek, Photoconductivity and Related Phenomena, edited by J. Mort and D. M. Pai, (Elsevier, Amsterdam, 1976)

9) S. O. Kasap and C. Juhasz: J. Phys. D: Appl. Phys., 18 (1985) 703.

10) J. Mort and G. Pfister, Electronic Properties of Polymers, edited by J. Mort and G. Pfister, (John Wiley and Sons, New York, 1982).

11) G. C. Hartmann and F. W. Schmidlin: J. Appl. Phys. 46 (1975) 266.

12) D. J. Gibbsons and A. C. Papadakis: J. Phys. Chem. Solids 29 (1968) 115.

13) I. Chen: Jpn. J. Appl. Phys. 28 (1989) 21.

14) K. Skarp, S. T. Lagerwall, and B. Stebler: Mol. Cryst. Liq. Cryst. 60 (1980) 215.

15) P. G. de Gennes, The Physics of Liquid Crystals, (Oxford, London, 1974), p.49.